Partial Breaking of Three-Fold Symmetry via Percolation of a Domain Wall

Soumyadeep Bhattacharya* and Purusattam Ray†
The Institute of Mathematical Sciences, CIT Campus, Taramani, Chennai 600113, India
(Dated: August 23, 2016)

We show that suppression of vortex strings splits the order-disorder transition in the three-state Potts ferromagnet on a simple cubic lattice and opens up an intermediate phase characterized by partial breaking of the three-fold symmetry and long-range order. In contrast, suppression of vortices in the same model on a square lattice results in an intermediate phase with enhanced U(1) symmetry and quasi-long-range order. We show that the difference between the two phases originates from distinct patterns of domain wall proliferation. A domain wall, separating the two most populous spin states, percolates on its own in the former phase but remains at a percolation threshold in the latter.

arXiv:1608.05901v1 [cond-mat.stat-mech] 21 Aug 2016

The spontaneous breaking of a three-fold symmetry in three dimensions is of crucial significance in high energy and condensed matter physics. The phase transition in the 3+1-dimensional $SU(3)$ gauge theory, which models the deconfinement of quarks and gluons to a plasma state, is effectively described by the transition in a three-dimensional spin model possessing a three-fold global symmetry [1]. The formation of cosmic strings across a phase transition during cooling of the early universe is captured by a model in which the phase of the Higgs field is discretized to three angles [2]. The three-fold symmetry breaking also captures the behavior of the valence-bond-solid order parameter across deconfined quantum phase transitions in the Heisenberg antiferromagnet on a honeycomb lattice [3, 4]. The phase transitions in these seemingly disparate systems share a common feature: they are accompanied by the proliferation of vortex defects.

Proliferation of topological defects is the underlying mechanism which drives phase transitions in a variety of systems possessing continuous symmetries [5–7]. The superfluid-normal phase transition, in particular, is driven by the proliferation of vortex defects [8–11]. Does proliferation of these defects drive the three-fold symmetry breaking transition as well? The vortex defects need not be solely responsible for driving the transition. Recently, we have shown that the three-fold symmetry, which is broken in the ordered phase of the two-dimensional three-state Potts model, is restored in the disordered phase by a simultaneous proliferation of vortices and domain walls [12]. When the core energy of vortices in that model is increased beyond a certain value, the simultaneous proliferation decouples and the vortices proliferate after the domain walls. This decoupling splits the order-disorder transition into two and leads to the appearance of an intermediate phase in which the three-fold symmetry enhances to U(1). Does the same behavior carry over to the three-dimensional model as well? Emergence of U(1) symmetry in three dimensions is topic of debate [13–19]. A direct demonstration of such an intermediate phase would not only help settle the debate but also have fascinating consequences in the physics of gauge theories and quantum condensed matter systems effectively described by a three-fold symmetry.

In this paper, we demonstrate that the order-disorder transition in the three-state Potts ferromagnet on a simple cubic lattice is driven by the simultaneous proliferation of vortex strings and domain walls. When we increase the core energy of vortex string segments, the transition continues to be driven by the coupled proliferation of the defects but shifts to a higher temperature. Increasing the core energy beyond a certain value decouples the simultaneous proliferation and splits the transition, resulting in the formation of an intermediate phase. The intermediate phase in this case, however, does not exhibit emergence of U(1) symmetry. Instead, it exhibits partial symmetry breaking. The intermediate phase in both two and three dimensions results from the proliferation of domain walls. How can the same defect driven mechanism produce two different types of phases? In order to find the distinguishing feature between the two proliferation patterns, we focus on the percolation properties of the domain walls. We find that one particular type of domain wall percolates on its own in the intermediate phase of the three-dimensional model while that same type of domain wall appears to remain at a percolation threshold throughout the intermediate phase of the two-dimensional model. Our result establishes that the nature of phases formed by domain wall proliferation can crucially depend on the percolation behavior of individual types of domain walls.

In order to list the types of domain walls sustained by the model, we place three-state spins $s_i \in \{0, 1, 2\}$ at each vertex i of a lattice Λ. In this work, we consider the model on a simple cubic lattice and on a square lattice. The domain walls and vortices reside on the dual lattice Λ', which in the case of the two types of integer lattices is also an integer lattice, but shifted from Λ by half a lattice spacing along each axis. The domain walls are defects with codimension one. For the simple cubic lattice, they appear on the plaquettes of Λ' which separate a pair of spins in dissimilar states. For the square lattice, the domain walls reside on the edges of Λ' [12].

Vortices are defects with codimension two. On the

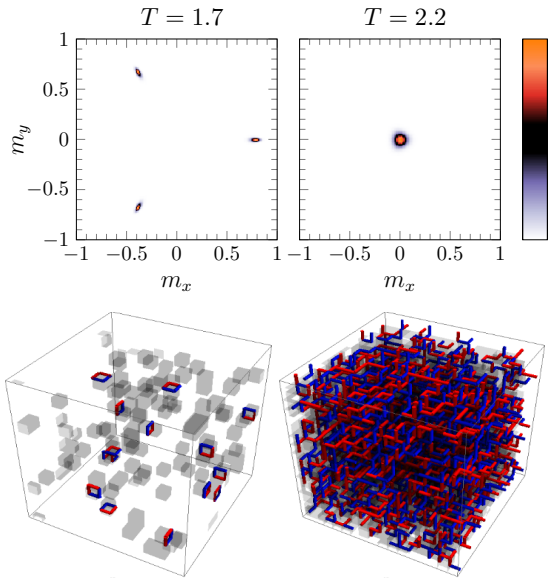

FIG. 1. Top panel shows the distribution of the three-fold vector order parameter obtained for a $L = 12$ system and bottom panel shows typical configurations of domain walls (gray), vortex (blue) and antivortex (red) strings at two different temperatures: (left) in the ordered phase at $T = 1.7$ and, (right) in the disordered phase at $T = 2.2$.

square lattice, they reside on the vertices $i' \in \Lambda'$. Each vertex i' is assigned a winding number $\omega_{i'} = (\Delta_{ba} + \Delta_{cb} + \Delta_{dc} + \Delta_{ad})/3$, where Δ_{ba} represents the state difference $(s_b - s_a)$ wrapped to lie in $[-1, +1]$ and s_a, s_b, s_c, s_d are the spin states at the four corners of the square plaquette in Λ surrounding i'. For the simple cubic lattice, the vortex string segments reside on the edges $e' \in \Lambda'$ and the winding number $\omega_{e'}$ is calculated using the same formula but with the spin states at the four corners of the square plaquette in Λ surrounding e' [20]. The vortex defects are absent when $\omega = 0$. A vortex or an antivortex is present when $\omega > 0$ or $\omega < 0$, respectively. The core energy of the vortices can be increased by associating an energy cost λ to each element of the dual lattice which contains a non-zero winding number [10, 12, 20–22].

The three-state Potts model on the simple cubic lattice with nearest-neighbor interaction between spins and a λ increment of vortex core energy is described by the Hamiltonian

$$\mathcal{H} = -\sum_{\langle i,j \rangle \in \Lambda} \delta(s_i, s_j) + \lambda \sum_{e' \in \Lambda'} |\omega_{e'}| \qquad (1)$$

We have simulated this model on a lattice with edge length L at different values of λ and temperature T using a single spin-flip algorithm [23]. At each temperature, we have initialized the system with a completely ordered spin configuration, discarded the first 10^4 uncorrelated configurations for equilibriation and measured observables over the next 10^5 uncorrelated configurations. In order to capture the macroscopic symmetry manifested by the model at different temperatures, we have measured the three-fold vector order parameter (m_x, m_y), where $m_x = L^{-3} \sum_{i \in \Lambda} \cos(2\pi s_i/3)$ and $m_y = L^{-3} \sum_{i \in \Lambda} \sin(2\pi s_i/3)$.

In the absence of core energy increment ($\lambda = 0$), the model exhibits a single order-disorder transition at $T = 1.81$ [24]. The order parameter distribution obtained from our simulation clearly shows a breaking of the three-fold symmetry in the ordered phase and its restoration in the disordered phase (Fig. 1). In addition, we find that both domain walls and vortex strings proliferate in the disordered phase while neither of them do so in the ordered phase.

In order to capture the proliferation behavior in a more quantitative manner, we have measured the density of the domain walls ρ_{dw}, defined as the fraction of plaquettes in Λ' separating dissimilar spin states, and the density of vortex strings ρ_{vx}, defined as the fraction of edges in Λ' that are assigned a non-zero winding number. For $\lambda = 0$, we find that the densities of both types of defects rise simultaneously across $T \approx 1.8$ (Fig. 2). The corresponding thermodynamic transition is captured by a decay in the magnetization $|m| = \sqrt{m_x^2 + m_y^2}$ across that temperature. In order to capture the possibility of symmetry enhancement, we have measured the strength of three-fold symmetry breaking using the observable $m_{3\phi} = \langle \cos 3\phi \rangle$, where $\phi = \arctan(m_y/m_x)$ is the angle of the order parameter [25]. The three-fold symmetry is broken in the ordered phase, which is confirmed by observing that $\langle \cos 3\phi \rangle = 1$ for $T < 1.8$ (Fig. 2). In the disordered phase both $\langle |m| \rangle$ and $\langle \cos 3\phi \rangle$ decay to zero. If the three-fold symmetry enhances to U(1), ϕ would fluctuate uniformly between 0 and 2π. This would result in $\langle \cos 3\phi \rangle = 0$ while the magnetization remains non-zero.

We begin to gradually increment the core energy in order to delay the proliferation of the vortex strings and decouple the simultaneous proliferation. For $\lambda = 0.4$, we find that the density of vortex strings and domain walls continue to rise together but at a higher temperature $T = 2.2$ (Fig. 2). This forces the order-disorder transition to shift to a higher temperature, as indicated by the change in the location at which the magnetization and $\langle \cos 3\phi \rangle$ decay. We find that the temperature of simultaneous defect proliferation and the temperature of the order-disorder transition continues to shift in this manner upto $\lambda \sim 1.4$. Up till this value, the suppression of vortex strings is too weak to decouple the proliferation. Above this value, we being to observe the first signs of decoupling.

For $\lambda = 1.5$, we find that the vortex string density rises at a temperature slightly higher than that of the domain walls (Fig. 2). The most prominent change, however, is visible in the behavior of $\langle \cos 3\phi \rangle$. Across an intermediate range of temperatures, starting at $T \approx 3$ and ending with the decay of magnetization at $T = 4.5$,

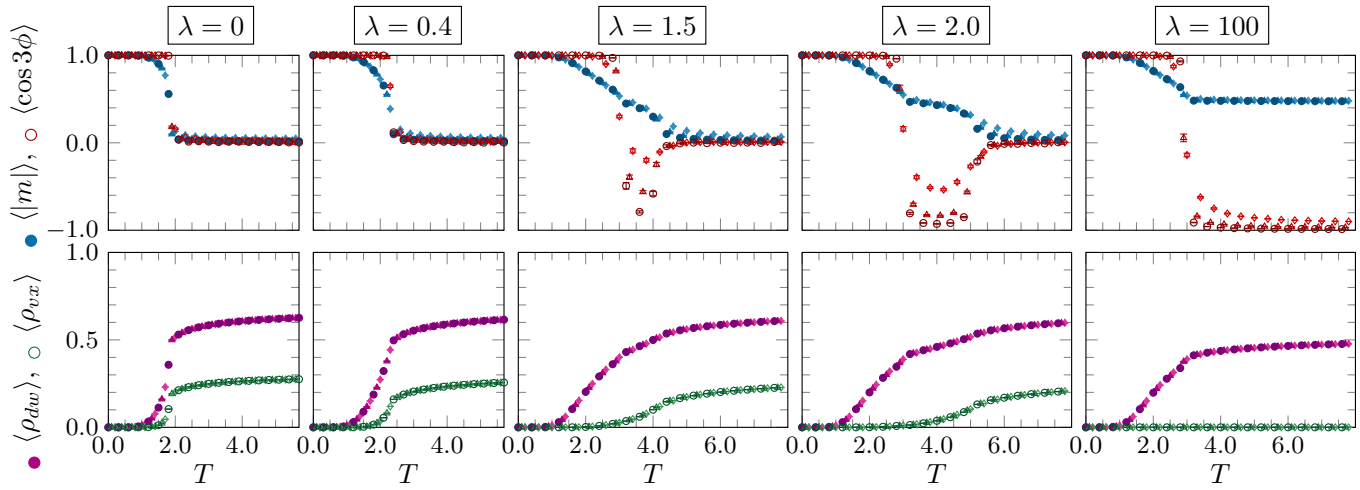

FIG. 2. The order-disorder transition, in the model without increment in vortex core energy λ, is marked by a decay of the magnetization $|m|$ and accompanied by a simultaneous rise in the density of domain walls ρ_{dw} and the density of vortex strings ρ_{vx}. For small values of λ, the defect densities rise and the magnetization decays at a higher temperature. For large values of λ, the vortex string density begins to rise at a temperature higher than that of domain wall density. The magnetization shows a two-step decay indicating the appearance of an intermediate phase. In the intermediate phase, the measure of three-fold symmetry breaking $\langle \cos 3\phi \rangle$ turns negative.

we find that $\langle \cos 3\phi \rangle$ goes negative. With increasing λ, the decay of magnetization, marking the transition from the intermediate phase to the disordered phase, continues to shift to higher temperatures following the shift in the proliferation temperature of vortex strings. For extreme suppression of the vortex strings using $\lambda = 100$, the intermediate-disorder transition recedes to very high temperatures and the intermediate region increases in extent. The transition from the ordered phase to the intermediate phase is accompanied by a rise in the density of domain walls. This transition remains at $T \approx 3$, unaffected by the increased suppression of vortex strings. This result clearly demonstrates that the intermediate-disorder transition is driven by the proliferation of vortex strings while the order-intermediate transition is driven by the proliferation of domain walls. This result is also a source of concern.

When the proliferation of vortices in the two-dimensional three-state Potts model is delayed by raising the core energy of vortices, the order-disorder transition splits and opens up an intermediate phase in a similar manner [12]. In that case, however, the intermediate phase exhibits enhancement of the three-fold symmetry to U(1). The intermediate phase in the present model shows a breaking of the three-fold symmetry at angles $\{\pi/3, \pi, 5\pi/3\}$ (Fig. 3), which results in negative values of $\langle \cos 3\phi \rangle$. In two dimensions, the emergent U(1) symmetry destroys long-range order in the intermediate phase [12]. This forces the system to quasi-long-range order, due to which the magnetization gradually decays to zero with increasing system size. In the intermediate phase of the three-dimensional model, the magnetization remains unchanged with system size but takes up an intermediate value $\langle |m| \rangle = 0.5$. This suggests that the system is partially ordered in that phase (Fig. 2). The onset of a partial order is expected because typical configurations obtained in that phase show that domain walls proliferate (Fig. 3) and allow the system to fragment into multiple domains which belong to different spin states. However, the quasi-long-range ordered phase in two dimensions is also formed due to the proliferation of domain walls [12]. How does the same defect-driven mechanism result in the formation of two different types of ordered phases? Since vortex defects are absent in the intermediate phase for both cases (Fig. 3), it is clear that they do not play a role in determining the nature of the phase. The distinguishing feature between the phase in the two cases must, therefore, lie in the pattern of domain

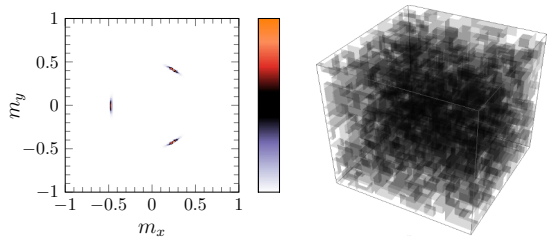

FIG. 3. Distribution of the order parameter, obtained for a $L = 12$ system in the intermediate phase with $\lambda = 100$ and $T = 6.0$, is shown on the left. A typical defect configuration obtained at the same temperature (right) shows that domain walls span across the system while vortex strings are absent. Data has been obtained for $L = 8$ (diamond), $L = 12$ (triangle) and $L = 16$ (circle).

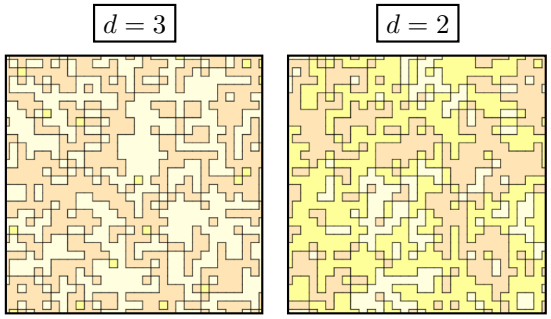

FIG. 4. Typical spin configurations obtained in the intermediate phase uncovered by extreme suppression of vortex defects with $\lambda = 100$ for the model on (left) a simple cubic lattice at $T = 6$, for which a two dimensional slice is shown here, and (right) a square lattice at $T = 4$. Domain walls are overlaid in black and vortex defects are found to be absent.

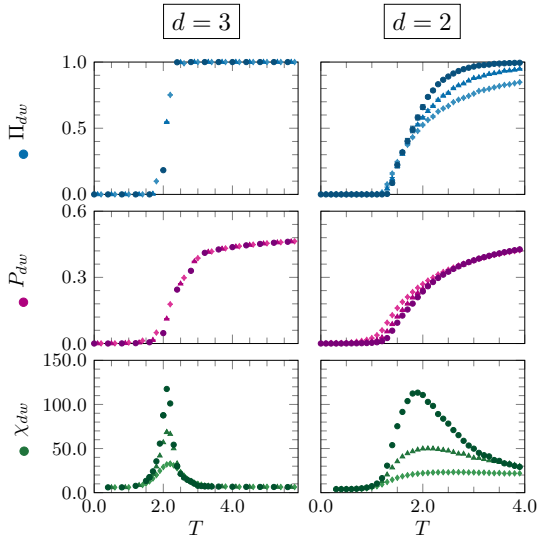

FIG. 5. Variation of standard percolation observables for domain walls with temperature in (left) the model on a simple cubic lattice and (right) the model on a square lattice with $\lambda = 100$. System sizes correspond to those in Fig. 2.

wall proliferation alone. However, the density of domain walls is clearly not a sufficient quantity for identifying the relevant pattern.

A visual inspection of typical spin configurations obtained in the intermediate phase of the two and three-dimensional models reveals a marked difference. In the configuration of the three-dimensional model (Fig. 4), we find that the numerous domains mostly belong to two of the three spin states. This implies that the proliferation of the domain walls can be further specified as a proliferation of domain walls separating the two spin states. This, however, is not the case for the two-dimensional model (Fig. 4). In the configuration obtained for that model, all the three spin states are present. Although the domain walls appear to span across the system, a particular type of domain wall, separating any of the two states, appears less likely to span across the system. Our inspection suggests that the distinguishing feature in the proliferation pattern resides in the percolation properties of particular types of domain walls.

We have measured standard percolation observables [26] for each type of domain wall in the model on both simple cubic and square lattices. A domain wall, which separates a pair of spin states a and b, is assigned a type $(a|b)$. As the model under considertaion is ferromagnetic, $(a|a)$ does not represent a domain wall. In addition, $(a|b)$ is equivalent to $(b|a)$, as the interaction between spins is non-chiral. In order to measure the percolation observables for $(a|b)$ domain walls, we have joined the $(d-1)$-dimensional $(a|b)$ domain wall segments on the d-dimensional dual lattice Λ' only if they share a $(d-2)$-dimensional element of Λ'. This criterion specializes to sharing of a dual edge in the three-dimensional case and the sharing of a dual vertex in the two-dimensional case. We have distinguished between separate components of $(a|b)$ domain walls by labelling them using the Hoshen-Kopelman alogrithm [26]. For each configuration, we have identified the largest domain wall of a particular type $(a|b)$ and measured the fraction $P_{dw(a|b)}$ of $(d-1)$-dimensional elements belonging to that domain wall. We have binned the sizes of the remaining $(a|b)$ domain walls into a distribution $n_{dw(a|b)}(s)$ and calculated the average size of $(a|b)$ domain walls as [26]

$$\chi_{dw(a|b)} = \frac{\sum_s s^2 n_{dw(a|b)}(s)}{\sum_s s n_{dw(a|b)}(s)} \tag{2}$$

For each configuration, we have also checked if at least one $(a|b)$ domain wall spans across the system from a face to its opposite face, under open boundary conditions. The average of this Boolean measurement over multiple configurations gives the spanning probability $\Pi_{dw(a|b)}$. We have also measured these observables for domain walls constructed irrespective of the particular type and labelled them as P_{dw}, χ_{dw} and Π_{dw}.

We find that Π_{dw} rises from zero in the ordered phase and saturates to unity is the intermediate phase of both the two and three-dimensional models (Fig. 5). In both cases, the percolation strength P_{dw} rises across the transition from the ordered phase to the intermediate phase and the average size of domain walls peaks with increasing system size near the transition in both cases. Although the variation in the percolation observables appear sharper in the case of the three-dimensional model, they exhibit qualitatively similar behavior in the two cases. While our result confirms that the domain walls percolate in the intermediate phase of both models, it suggests that the percolation properties of the domain walls, irrespective of the particular type, cannot be used to distinguish between the proliferation pattern in the two cases.

Before presenting the percolation properties for $(a|b)$ domain walls, we mention a feature of Monte Carlo simulations that needs to be taken into consideration in order to obtain accurate results for this particular set of observables. All the observables which we have measured previously are invariant under the symmetry operations of the $\mathbb{Z}_3$ symmetry group. For example, if all the spins in a given configuration are rotated by $2\pi/3$, the values of observables like magnetization, $\langle \cos 3\phi \rangle$ and even the density of the defects remain invariant. On the other hand, observables like the percolation strength of $(0|1)$ domain walls depends on specific states and, therefore, do not remain invariant under a global rotation of the spins. This becomes a problem in finite size simulations because the system keeps migrating from one symmetry broken minima to the other over the course of the simulation [14]. We have mitigated this problem by rotating all the spins by an angle such that the angle of the symmetry broken minima gets relabelled to 0 (state 0). Since discrete rotations are constituent members of the $\mathbb{Z}_3$ symmetry group, this procedure of relabelling keeps the Hamiltonian (eq. 1) invariant. However, this relabelling is not sufficient. Even if we fix the symmetry broken minima, the system can fluctuate between the angles on the left and right hand side of angle 0 (state 0). In order to counter such fluctuations, we reflect all the spins in the configuration across angle 0, in a manner such that the most populous of the two angles gets relabelled to angle $2\pi/3$ or state 1. Consequently, the angle on the other side gets relabelled to $4\pi/3$ or state 2. Again, this reflection operation is a constituent member of the $\mathbb{Z}_3$ symmetry group and, therefore, keeps the Hamiltonian (eq. 1) invariant.

We have applied the relabelling scheme to every configuration generated in our simulation before measuring the percolation observables for $(a|b)$ domain walls. Under this relabelling, domain walls of type $(0|1)$ separate spins belonging to the two most populous states. we find that the $(0|1)$ domain walls begin to percolate on their own across the transition from the ordered phase to the intermediate phase in three dimensions (Fig. 6). The spanning probability of this particular type saturates to unity in the latter phase and the average size of $(0|1)$ domain walls peaks at the transition. As expected from the visual inspection (Fig. 4), none of the other types of domain walls, $(0|2)$ and $(1|2)$, are found to percolate on their own across the transition.

In the intermediate phase of the two-dimensional model, however, we find that the $(0|1)$ domain walls show a different behavior. The spanning probability does not saturate to unity but remains at $\Pi_{dw(0|1)} \approx 0.5$ (Fig. 6). The percolation strength of $(0|1)$ domain walls gradually decreases with increasing system size at each temperature in the phase. In addition, the average size of $(0|1)$ domain walls not only peaks at the transition but continues to grow with system size at each temperature in the the

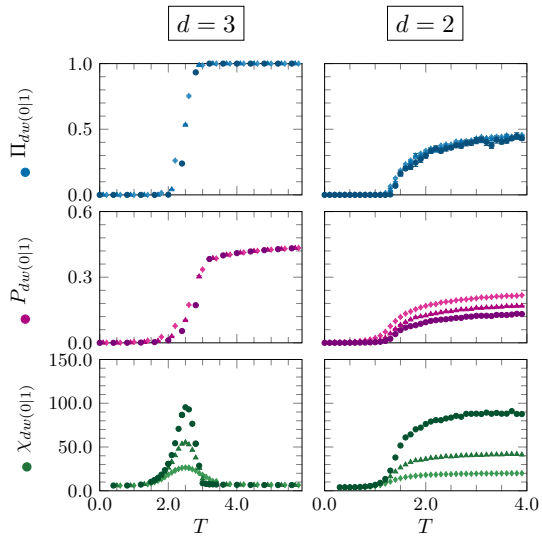

FIG. 6. Variation of standard percolation observables for $(0|1)$ domain walls with temperature in (left) the model on a simple cubic lattice and (right) the model on a square lattice with $\lambda = 100$. System sizes correspond to those in Fig. 2.

phase. The percolation behavior exhibited at each temperature in the phase is usually observed only that the threshold of a percolation transition [26]. This implies that the $(0|1)$ domain walls do not percolate on their own in the intermediate phase of the two-dimensional model, but remain at a percolation threshold throughout the phase. We have found that none of the other types of domain walls show percolation or threshold behavior in the intermediate phase.

Our result establishes that the percolation of the $(0|1)$ domain walls is the salient feature which distinguishes the intermediate phase of the three-dimensional model from that of its two-dimensional counterpart. This feature also explains the pattern of symmetry breaking obtained in the intermediate phase of the three-dimensional model. The percolation of $(0|1)$ domain walls implies a percolation of state 0 clusters and state 1 clusters. This, in turn, implies a spin texture dominated by angles 0 and $2\pi/3$ in equal proportion. Consequently, the average orientation of the system becomes $\pi/3$. As the simulation progresses, the symmetry broken minima shifts across the other two angles as well. Therefore, we obtain the $\pi/3$ offset pattern of three-fold symmetry breaking in the ordered parameter distribution for this phase (Fig. 3). Another way to look at the same result is that state 0 and state 1 act like the two states of a $\mathbb{Z}_2$ Ising model. In the ordered phase, most of the spins are in state 0, because of which the Ising symmetry remains broken. In the intermediate phase, most of the spins arbitrarily pick up on of the two states. Therefore, the Ising symmetry gets restored, the symmetry of the system remains only partially broken and the spins exhibit a partial order instead of complete order. We note that this partial order is similar

to the up-down-up-down height profile of layers grown in the disordered-flat phase of crystal growth [27, 28]. This type of partial order has also been reported for $\mathbb{Z}_4$ models in three dimensions and is termed as a $\langle\sigma\rangle$ phase in the literature for the Ashkin-Teller model [29, 30].

The crucial difference between the two-dimensional and three-dimensional behavior lies in the fact that simultaneous percolation of multiple clusters (also known as polychromatic percolation) can be sustained by the simple cubic lattice, due to its higher connectivity, but not by the square lattice [35]. Since the two-dimensional system cannot accomodate the simultaneous percolation of state 0 and state 1 clusters, and yet the temperature is ripe for domain wall proliferation, the (0|1) domain walls do not percolate but remain only at a percolation threshold. While the threshold behavior in two dimensions has not been reported before, the percolation behavior in three dimensions has been discussed in the context of a six-state model [28].

The six-state clock model, with a generalized interaction potential, exhibits a similar intermediate phase in which the six-fold symmetry is broken at angles offset from the symmetry breaking pattern in the ordered phase by $\pi/6$ [31, 32]. This pattern is captured by $\langle\cos 6\phi\rangle$ going negative in that phase. It has been suggested that a variety of intermediate phases in three-dimensional $\mathbb{Z}_n$ models can be distinguished from each other via the percolation properties of stochastically reduced spin and bond clusters [28, 33, 34]. In particular, it has been suggested that the intermediate phase with negative $\langle\cos n\phi\rangle$ is characterized by the percolation of a reduced cluster of bonds separating spins which differ by one state [28]. Such clusters are the stochastically reduced counterparts of the geometric domain walls that we have considered here. We have shown that a single type of geometric domain wall percolates on its own in the intermediate phase of the $\mathbb{Z}_3$ model. It would be interesting to verify if the percolation is sustained after the stochastic reduction. We note, however, that the suppression effect produced by the λ term in the Hamiltonian (eq. 1) would be quite difficult to factor into the scheme for stochastic reduction [28, 33] as it contains a plaquette-based evaluation of the winding number.

* sbhtta@imsc.res.in
† ray@imsc.res.in

[1] B. Svetitsky and L. G. Yaffe, Nucl. Phys. B **210** 423, (1982).
[2] T. Vachaspati and A. Vilenkin, Phys. Rev. D **30** 2036, (1984).
[3] R. Ganesh R., J. van den Brink and S. Nishimoto, Phys. Rev. Lett. **110** 127203, (2013).
[4] S. Pujari, K. Damle and F. Alet, Phys. Rev. Lett. **111** 087203 (2013).
[5] N. D. Mermin, Rev. Mod. Phys. **51** 591 (1979).
[6] P. M. Chaikin and T. C. Lubensky *Principles of Condensed Matter Physics* (Cambridge University Press, 2000).
[7] A. Vilenkin and E. P. S. Shellard, *Cosmic Strings and Other Topological Defects* (Cambridge University Press, 2000).
[8] V. L. Berezinskii, Sov. Phys. JETP **32** 493 (1971).
[9] J. M. Kosterlitz and D. J. Thouless, J. Phys. C **6** 1181 (1973).
[10] G. Kohring, R. E. Shrock and P. Wills, Phys. Rev. Lett. **57** 1358 (1986).
[11] G. A. Williams, Phys. Rev. Lett. **82** 1201 (1999).
[12] S. Bhattacharya and P. Ray, Phys. Rev. Lett. **116** 097206 (2016).
[13] D. Blankschtein, M. Ma, A. N. Berker, G. S. Grest and C. M. Soukoulis, Phys. Rev. B **29** 5250 (1984).
[14] S. Miyashita J. Phys. Soc. Jpn. **66** 3411 (1997).
[15] M. Oshikawa Phys. Rev. B **61** 3430 (2000).
[16] J. Lou, A. W. Sandvik and L. Balents Phys. Rev. Lett. **99** 207203 (2007).
[17] C. Maes and S. Shlosman, J. Stat. Phys. **144** 1238 (2011).
[18] A. C. D. Van Enter, C. Kulske and A. A. Opoku, J. Phys. A **44** 475002 (2011).
[19] O. Borisenko, V. Chelnokov, G. Cortese, M. Gravina, A. Papa and I. Surzhikov, arXiv:1311.0471 [hep-lat] (2013).
[20] E. Bittner, A. Krinner and W. Janke, Phys. Rev. B **72** 094511 (2005).
[21] S. R. Shenoy Phys. Rev. B **42** 8595 (1990).
[22] S. Sinha and S. K. Roy, Phys. Rev. E **81** 041120 (2010).
[23] D. P. Landau and K. Binder, *A Guide to Monte Carlo Simulations in Statistical Physics* (Cambridge University Press, 2014).
[24] W. Janke and R. Villanova, Nucl. Phys. B **489** 679 (1997).
[25] S. K. Baek, P. Minnhagen and B. J. Kim, Phys. Rev. E **80** 060101 (2009).
[26] D. Stauffer and A. Aharony, *Introduction to Percolation Theory* (CRC press, 1994).
[27] P. B. Weichman and A. Prasad, Phys. Rev. Lett. **76** 2322 (1996).
[28] Y. Ueno, J. Stat. Phys. **80** 841 (1995).
[29] R. V. Ditzian, J. R. Banavar, G. S. Grest and L. P. Kadanoff, Phys. Rev. B **22** 2542 (1980).
[30] P. Pawlicki, G. Kamieniarz and L. Debski, Physica A **242** 290 (1997).
[31] N. Todoroki, Y. Ueno and S. Miyashita, Phys. Rev. B **66** 214405 (2002).
[32] Y. Ueno and K. Kasono, Phys. Rev. B **48** 16471 (1993).
[33] L. Chayes and J. Machta, Physica A **239** 542 (1997).
[34] L. Chayes, D. McKellar and B. Winn, J. Phys. A **31** 9055 (1998).
[35] R. Zallen Phys. Rev. B **16** 1426 (1977).